

## Enhancement and control of carrier lifetimes in p-type 4H-SiC epilayers

T. Hayashi, K. Asano, J. Suda, and T. Kimoto

Citation: *J. Appl. Phys.* **112**, 064503 (2012); doi: 10.1063/1.4748315

View online: <http://dx.doi.org/10.1063/1.4748315>

View Table of Contents: <http://jap.aip.org/resource/1/JAPIAU/v112/i6>

Published by the [American Institute of Physics](#).

---

### Additional information on *J. Appl. Phys.*

Journal Homepage: <http://jap.aip.org/>

Journal Information: [http://jap.aip.org/about/about\\_the\\_journal](http://jap.aip.org/about/about_the_journal)

Top downloads: [http://jap.aip.org/features/most\\_downloaded](http://jap.aip.org/features/most_downloaded)

Information for Authors: <http://jap.aip.org/authors>

## ADVERTISEMENT



**AIP Advances**

Now Indexed in  
Thomson Reuters  
Databases

Explore AIP's open access journal:

- Rapid publication
- Article-level metrics
- Post-publication rating and commenting

## Enhancement and control of carrier lifetimes in p-type 4H-SiC epilayers

T. Hayashi,<sup>1,2</sup> K. Asano,<sup>2</sup> J. Suda,<sup>1</sup> and T. Kimoto<sup>1</sup>

<sup>1</sup>Department of Electronic Science and Engineering, Kyoto University, Kyotodaigaku-katsura, Nishikyo, Kyoto 615-8510, Japan

<sup>2</sup>Power Engineering R&D Center, Kansai Electric Power Co., Inc. 3-11-20 Nakoji, Amagasaki 661-0974, Japan

(Received 10 April 2012; accepted 25 July 2012; published online 17 September 2012)

Enhancement and control of carrier lifetimes in p-type 4H-SiC have been investigated. In this study, thermal oxidation and carbon ion implantation methods, both of which are effective for lifetime enhancement in n-type SiC, were attempted on 147- $\mu\text{m}$  thick p-type 4H-SiC epilayers. Effects of surface passivation on carrier lifetimes were also investigated. The carrier lifetimes in p-type SiC could be enhanced from 0.9  $\mu\text{s}$  (as-grown) to 2.6  $\mu\text{s}$  by either thermal oxidation or carbon implantation and subsequent Ar annealing, although the improvement effect for the p-type epilayers was smaller than that for the n-type epilayers. After the lifetime enhancement, electron irradiation was performed to control the carrier lifetime. The distribution of carrier lifetimes in each irradiated region was rather uniform, along with successful lifetime control in the p-type epilayer in the range from 0.1 to 1.6  $\mu\text{s}$ . © 2012 American Institute of Physics. [<http://dx.doi.org/10.1063/1.4748315>]

### I. INTRODUCTION

Silicon carbide (SiC) has received increasing attention as a next-generation semiconductor material for realizing high-power, high-temperature, and high-frequency devices, due to such outstanding physical properties as wide bandgap, high breakdown field strength, and superior thermal conductivity.<sup>1,2</sup> 4H-SiC has been regarded as the most promising polytype for vertical-type high-voltage devices, given its higher bulk mobility and smaller anisotropy. Ultrahigh-voltage SiC devices—bipolar power devices in particular—are suitable for high-power electrical conversion systems, where the material properties of SiC offer significant advantages over those of conventional Si devices. High-voltage bipolar devices require a long carrier lifetime to modulate the conductivity of very thick voltage-blocking layers. Conversely, a short carrier lifetime inhibits effective conductivity modulation and prevents low on-resistance from being attained.

The carrier lifetimes typically observed in SiC had been short, approximately 1  $\mu\text{s}$ , thus marking a few orders of magnitude lower than that of high-purity silicon. This subject has, therefore, been extensively investigated.<sup>3</sup> With respect to the relation between carrier lifetime and deep levels, Tawara *et al.* and Klein *et al.* have reported that the  $Z_{1/2}$  ( $E_C - 0.65$  eV) centers influence the carrier lifetimes of 4H-SiC epilayers.<sup>4,5</sup> Danno *et al.* revealed the clear relation between the carrier lifetime and the  $Z_{1/2}$  and/or  $\text{EH}_{6/7}$  ( $E_C - 1.55$  eV) centers in a wide range of the trap concentrations<sup>6</sup> and clarified that carrier lifetimes are limited by the  $Z_{1/2}$  and/or  $\text{EH}_{6/7}$  centers. They also found that carrier lifetimes are limited by other factors such as surface recombination at a sufficiently low  $Z_{1/2}$  concentration. Reshanov *et al.* and Klein *et al.* concluded that the  $\text{EH}_{6/7}$  center cannot be a lifetime killer after comparing the deep level transient spectroscopy (DLTS) spectra of a pn junction with and without minority-carrier injection.<sup>5,7</sup> In recent years, a few groups attempted reduction of these deep levels and successfully

improved carrier lifetimes. Storasta *et al.* have shown a dramatic reduction in the concentration of the  $Z_{1/2}$  center by using carbon ion implantation combined with subsequent diffusion via high-temperature annealing.<sup>8</sup> The authors' group has demonstrated elimination of these centers by thermal oxidation.<sup>9</sup> So far, the lifetime killers in n-type SiC have been systematically analyzed,<sup>10,11</sup> and long lifetimes of 9–19  $\mu\text{s}$  have been achieved.<sup>12,13</sup>

On the other hand, a too long lifetime will cause considerably large reverse recovery, leading to limited switching frequency and excessive switching loss. Therefore, the carrier lifetime should be controlled to achieve an optimum lifetime value and its profile. Danno *et al.* succeeded in achieving lifetime control for an n-type 4H-SiC epilayer by changing the  $Z_{1/2}$  concentration using electron irradiation.<sup>6</sup> However, these beneficial results have mainly addressed the n-type 4H-SiC, with very few reports on the carrier lifetimes in thick and lightly doped p-type SiC,<sup>14,15</sup> which is often employed as the voltage-blocking region of high-voltage SiC switching devices such as thyristors<sup>16</sup> and insulated gate bipolar transistors (IGBTs).<sup>17</sup>

In this work, the authors attempted to enhance carrier lifetimes in p-type 4H-SiC by employing thermal oxidation or carbon implantation, each of which is effective for lifetime enhancement in n-type SiC. The authors consequently confirmed enhancement of carrier lifetimes in p-type SiC by thermal oxidation as well as carbon implantation and subsequent annealing. In order to control the carrier lifetime, electron irradiation was carried out after the lifetime enhancement. As a result, a carrier lifetime in the range from 0.1 to 1.6  $\mu\text{s}$  was obtained.

### II. EXPERIMENT

The samples employed in this study were aluminum-doped, p-type epilayers grown on 8° off-axis 4H-SiC (0001) substrates by chemical vapor deposition (CVD). The doping concentration was  $5.6 \times 10^{14} \text{ cm}^{-3}$ . In this study, very thick

epilayers with 147  $\mu\text{m}$  in thickness were employed to minimize the influence of recombination in the substrate and/or interface.<sup>12,18,19</sup>

The carrier lifetimes of p-type 4H-SiC epilayers were measured by a microwave photoconductance decay ( $\mu$ -PCD) method at room temperature. The  $\mu$ -PCD method used in this study allows for contactless measurements of carrier lifetimes. In this measurement, a pulsed yttrium lithium fluoride (YLF)-3HG laser of 349-nm wavelength was used to generate excess carriers. Decay in electrical conductivity (proportional to the excess carrier concentration) was monitored with microwave reflectivity at a frequency of 26 GHz. This method has been employed as a standard technique for measuring the lifetimes of Si.<sup>20</sup> In order to increase the signal-to-noise ratio of  $\mu$ -PCD signals, this study employed a differential  $\mu$ -PCD method that monitors differences in microwave reflectivity from areas with and without laser illumination. The concentration of generated carriers was calculated by using the absorption coefficient at this wavelength ( $\alpha = 324 \text{ cm}^{-1}$ ).<sup>21</sup> The typical concentration of generated carriers was  $1 \times 10^{15} \text{ cm}^{-3}$ . In the p-type epilayer, the hole concentration ( $p_0$ ) at room temperature is about  $2 \times 10^{14} \text{ cm}^{-3}$ , as estimated from the acceptor concentration and the ionization energy.<sup>22</sup> Because the background hole concentration is much lower than the generated carrier concentration, a high-injection level condition ( $\delta n = \delta p \gg p_0$ ) is almost satisfied, although it does not reach the high injection limit.

To improve carrier lifetimes in SiC, thermal oxidation was carried out at 1350  $^{\circ}\text{C}$  for reduction of deep levels.<sup>9</sup> After the thermal oxidation, hydrofluoric acid was used to remove the surface oxide film, and then the carrier lifetime was measured. After the measurement, high-temperature annealing was performed in Ar atmosphere at 1550  $^{\circ}\text{C}$  for 30 min with a carbon cap formed on the substrate surface, in order to reduce the HK0 center generated by thermal oxidation.<sup>23</sup> Surface passivation with deposited  $\text{SiO}_2$  followed by annealing in NO were then performed. Note that deposited  $\text{SiO}_2$  followed by annealing in NO yields a low interface state density and effectively suppresses surface recombination for n-type 4H-SiC.<sup>18,24</sup>

We also attempted reduction of deep levels in p-type SiC by using carbon implantation followed by high-temperature annealing. Tsuchida and co-workers proposed this method to successfully eliminate the  $Z_{1/2}$  center and enhance the carrier lifetime in n-type SiC.<sup>8,25</sup> The experimental conditions are as follows: Carbon ions were implanted at 600  $^{\circ}\text{C}$  to make a 300-nm deep box profile with a carbon concentration of  $5 \times 10^{20} \text{ cm}^{-3}$ . After implantation, samples were annealed in Ar at 1600–1800  $^{\circ}\text{C}$  for 30 min. Then 3  $\mu\text{m}$  of the surface region damaged by implantation was etched by using reactive ion etching (RIE), followed by rapid thermal annealing (RTA) in Ar at 1000  $^{\circ}\text{C}$  for 2 min to reduce deep levels generated by the etching process.<sup>26</sup>

Carrier lifetime control of the p-type 4H-SiC was conducted by employing electron irradiation. In this work, lifetime-enhanced epilayers were used as the starting material. Electron irradiation was performed at room temperature with irradiation energy of 200 keV or 400 keV. The electron

fluence was changed from  $5.0 \times 10^{15}$  to  $3.1 \times 10^{16} \text{ cm}^{-2}$  for 200 keV and from  $5.0 \times 10^{14}$  to  $2.7 \times 10^{15} \text{ cm}^{-2}$  for 400 keV, so as to vary the concentrations of generated deep levels. After irradiation, the samples were annealed by RTA in Ar at 1000  $^{\circ}\text{C}$  for 2 min.

### III. RESULTS

#### A. Lifetime enhancement

To improve carrier lifetimes, three process steps, (i) oxidation at 1350  $^{\circ}\text{C}$  for 10 h, (ii) subsequent Ar annealing at 1550  $^{\circ}\text{C}$ , and (iii) surface passivation with deposited  $\text{SiO}_2$  followed by annealing in NO were tried. Figure 1 shows the  $\mu$ -PCD decay curves measured before and after each processing step for a 147- $\mu\text{m}$  thick p-type epilayer. The obvious increment in carrier lifetime can be confirmed after each treatment. The lifetime was 0.9  $\mu\text{s}$  for the as-grown epilayer and reached 1.8  $\mu\text{s}$  after the surface passivation.

To clarify the role of each step, only surface passivation was performed on the 147- $\mu\text{m}$  thick as-grown epilayer. Figure 2 shows the  $\mu$ -PCD decay curves measured before and after only surface passivation treatment on the 147- $\mu\text{m}$  thick p-type epilayer. The surface passivation on as-grown epilayers gave virtually no impact on the  $\mu$ -PCD decay curves with the carrier lifetime about 1  $\mu\text{s}$ , indicating that the lifetimes of thick as-grown epilayers are indeed governed by bulk defects. Thus, the influence of surface recombination becomes significant when the bulk lifetime is long.

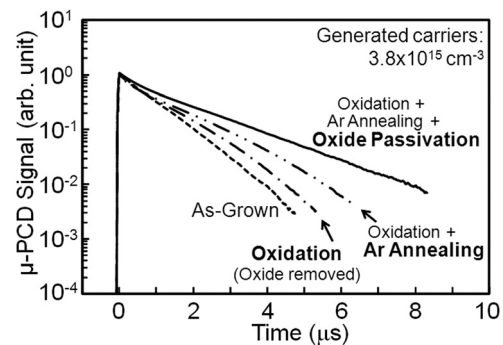


FIG. 1.  $\mu$ -PCD decay curves measured before and after various processing steps (oxidation at 1300  $^{\circ}\text{C}$  for 5 h, Ar annealing at 1550  $^{\circ}\text{C}$  for 30 min, and surface passivation with a nitrided oxide) for a 147- $\mu\text{m}$  thick p-type 4H-SiC epilayer.

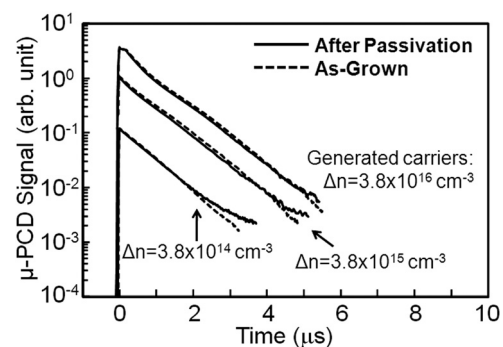


FIG. 2.  $\mu$ -PCD decay curves for a 147- $\mu\text{m}$  thick p-type 4H-SiC epilayer (as-grown) before and after surface passivation with deposited  $\text{SiO}_2$  annealed in NO.

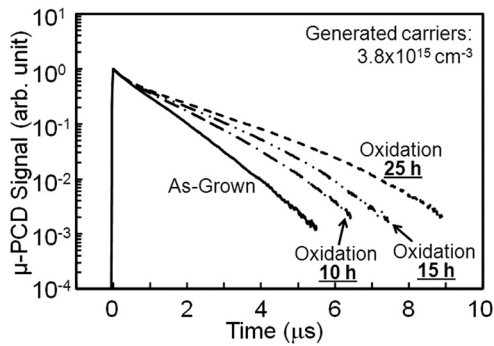


FIG. 3.  $\mu$ -PCD decay curves for a 147- $\mu\text{m}$  thick p-type 4H-SiC epilayer after oxidation at 1350 °C for 10, 15, and 25 h.

Then, only thermal oxidation was performed on the 147- $\mu\text{m}$  thick as-grown epilayer. Figure 3 shows the decay curves before and after dry oxidation at 1350 °C for 10, 15, and 25 h. The continuous increase in carrier lifetimes by longer oxidation is evident. The authors have revealed that the region with a reduced trap ( $Z_{1/2}$ ,  $\text{EH}_{6/7}$ , etc.) concentration becomes deeper as the oxidation time is increased in n-type 4H-SiC.<sup>9,27</sup> The result shown in Fig. 3 indicates that a similar phenomenon is taking place in p-type SiC, though the carrier lifetime killer in p-type 4H-SiC has not yet been identified. To further improve the lifetimes, the oxidation time was prolonged up to 45 h. Figure 4 shows the oxidation time dependence of carrier lifetime in the p-type epilayer with various oxidation times up to 45 h. The lifetime enhancement is effective in the early oxidation stage, but the effect is almost saturated after oxidation for 25 h. Although carrier lifetimes in p-type SiC reached 2.6  $\mu\text{s}$  by thermal oxidation at 1350 °C for 45 h and subsequent Ar annealing at 1550 °C for 30 min, it should be noted that the obtained carrier lifetime of the p-type SiC is considerably shorter than that of thick n-type SiC with a similar thickness ( $>9 \mu\text{s}$ ).<sup>12</sup>

Carbon implantation was then attempted on different as-grown samples, which were cut from the same epi-wafer as that described above. Figure 5 shows the annealing temperature dependence of carrier lifetime after carbon implantation in the 147- $\mu\text{m}$  thick p-type SiC. The lifetime was 0.9  $\mu\text{s}$  for the as-grown epilayer and reached 1.6  $\mu\text{s}$  after the process at an annealing temperature of 1700 °C. Although the carrier lifetime was enhanced by this method, the improvement effect is similar to that of the thermal oxidation process, and

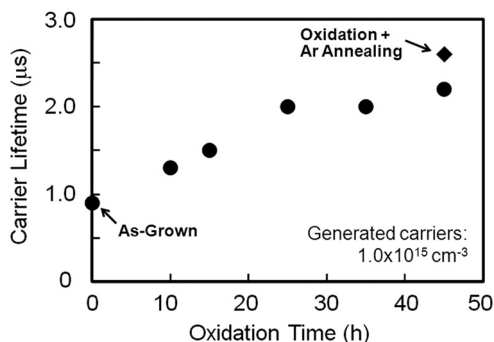


FIG. 4. Oxidation-time dependence of carrier lifetime for a 147- $\mu\text{m}$  thick p-type 4H-SiC epilayer with various oxidation times up to 45 h.

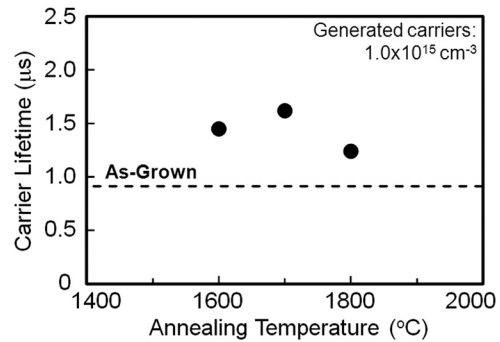


FIG. 5. Annealing temperature dependence of carrier lifetime in 147- $\mu\text{m}$  thick p-type 4H-SiC epilayers after carbon implantation process. Carbon ions were implanted at 600 °C to make a 300-nm deep box profile with a carbon concentration of  $5 \times 10^{20} \text{cm}^{-3}$ .

the carrier lifetimes were shorter than that in n-type SiC. As for the annealing temperature, the carrier lifetime exhibited a maximum value at an annealing temperature of about 1700 °C. There is an experimental fact that the concentration of the  $Z_{1/2}$  and  $\text{EH}_{6/7}$  centers increases when n-type 4H-SiC epilayers with relatively low concentration of  $Z_{1/2}$  center are annealed at very high temperature ( $>1750 \text{ °C}$ ).<sup>28,29</sup> If these defects dominantly limit the lifetime, it is predicted that a similar phenomenon will occur due to the high temperature annealing process (the concentration of the  $Z_{1/2}$  and  $\text{EH}_{6/7}$  center increases), causing the decrease of carrier lifetime, when the samples were annealed at very high temperature above 1700 °C. The generation of other defect centers in p-type SiC by high-temperature annealing should be also investigated in the future, in order to give a conclusive remark.

## B. Lifetime control

Bipolar devices require a long carrier lifetime for effective conductivity modulation. On the other hand, a too long lifetime can cause an excessive switching loss through large reverse recovery. Therefore, optimum lifetime values should be optimized by lifetime control processing. In this study, the authors attempted carrier lifetime control in p-type 4H-SiC epilayers by using electron irradiation. The samples used here were the lifetime-enhanced epilayers by employing the thermal oxidation described in the last subsection (Sec. III A). In terms of deep levels in as-grown SiC epilayers, the major deep levels are  $Z_{1/2}$  and  $\text{EH}_{6/7}$  centers in n-type<sup>11</sup> and HK2 ( $E_V + 0.84 \text{ eV}$ ), HK3 ( $E_V + 1.27 \text{ eV}$ ), and HK4 ( $E_V + 1.44 \text{ eV}$ ) centers in p-type epilayers.<sup>30</sup> The D ( $E_V + 0.49 \text{ eV}$ ) center related to boron is often confirmed in p-type epilayers.<sup>31</sup> Table I lists the deep levels existing in as-grown 4H-SiC epilayers and those after the electron irradiation followed by Ar annealing at 1000 °C. Various and high density deep levels are generated after electron irradiation is performed. However, after the Ar annealing process at 1000 °C, the  $Z_{1/2}$ ,  $\text{EH}_{6/7}$ , UK1 ( $E_V + 0.30 \text{ eV}$ ), UK2 ( $E_V + 0.58 \text{ eV}$ ), and HK4 centers will mainly remain in 4H-SiC epilayers.<sup>30</sup> In this case, the authors assumed that the same deep levels exist in the band gap for both p-type and n-type 4H-SiC. Since the formation energy of a point defect



TABLE I. Major deep levels existing in an as-grown 4H-SiC epilayer and those after the irradiation and annealing. (The same deep levels are assumed to exist in the band gap for both p-type and n-type 4H-SiC.)

Process	type	Label <sup>a</sup>	Position in the bandgap <sup>a</sup>
As-Grown	n	Z <sub>1/2</sub>	E <sub>C</sub> - 0.65 eV
		EH <sub>6/7</sub>	E <sub>C</sub> - 1.55 eV
	P	HK2	E <sub>V</sub> + 0.84 eV
		HK3	E <sub>V</sub> + 1.27 eV
		HK4	E <sub>V</sub> + 1.44 eV
After the electron irradiation and annealed in Ar at 1000 °C <sup>c</sup>	n	Z <sub>1/2</sub>	E <sub>C</sub> - 0.65 eV
		EH <sub>6/7</sub>	E <sub>C</sub> - 1.55 eV
	P	UK1	E <sub>V</sub> + 0.30 eV
		UK2	E <sub>V</sub> + 0.58 eV
		HK4	E <sub>V</sub> + 1 - 44 eV
(D) <sup>b</sup>	(E <sub>V</sub> + 0.49 eV)		

<sup>a</sup>Labels and positions of deep levels were adopted from Ref. 30 and 31.

<sup>b</sup>The deep level written within a parenthesis denotes that the defect density detected in the present samples was below  $1 \times 10^{12} \text{ cm}^{-3}$ .

<sup>c</sup>In case of using the lifetime-enhanced epilayer by employing the thermal oxidation and annealing as the starting material.

(vacancy, interstitial, antisite, etc.) generally depends on the position of Fermi level, the same defects do not always exist with a similar concentration in n- and p-type materials. Nevertheless, we assume the existence of some defects in n- and p-type 4H-SiC here for simplicity and discuss a candidate for a lifetime killer in p-type 4H-SiC. It should be also noted that the charge states of these defects also depend on the Fermi level, even if they exist. Further fundamental study on deep levels in n- and p-type 4H-SiC is required to make this discussion more complete.

Electron irradiations were performed at room temperature with irradiation energy of 200 keV or 400 keV. After irradiation, the samples were annealed in Ar at 1000 °C for 2 min to eliminate thermally unstable deep levels. To determine the irradiation conditions, we assumed that the generation rate of the Z<sub>1/2</sub> center by electron irradiation in p-type 4H-SiC is the same as that in n-type SiC. Our group has reported the relation between the irradiation energy of electrons and the generated-trap concentration per unit fluence for n-type 4H-SiC ( $6-8 \times 10^{-3} \text{ cm}^{-1}$  for 200 keV irradiation and  $7-8 \times 10^{-2} \text{ cm}^{-1}$  for 400 keV irradiation).<sup>32</sup> Table II

TABLE II. Electron fluence of the irradiation condition. The estimated Z<sub>1/2</sub> concentration is set from  $4 \times 10^{13}$  to  $2 \times 10^{14} \text{ cm}^{-3}$ .

Electron Fluence (cm <sup>-2</sup> )		
Irradiation energy	Irradiation energy	Estimated Z <sub>1/2</sub> Concentration (cm <sup>3</sup> )
200 keV	400 keV	
0	0	$< 1.0 \times 10^{12}$
$5.0 \times 10^{15}$	$5.0 \times 10^{14}$	$4.0 \times 10^{13}$
$7.9 \times 10^{15}$	-	$6.0 \times 10^{13}$
$1.3 \times 10^{16}$	$1.2 \times 10^{15}$	$9.0 \times 10^{13}$
$2.1 \times 10^{16}$	-	$1.4 \times 10^{14}$
$3.1 \times 10^{16}$	$2.7 \times 10^{15}$	$2.0 \times 10^{14}$

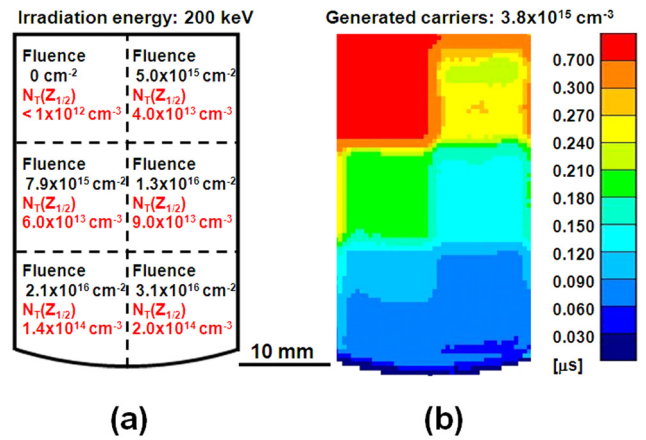


FIG. 6. Distribution of carrier lifetimes in a p-type 4H-SiC sample after the lifetime control process with irradiation energy of 200 keV: (a) irradiation condition and (b) lifetime mapping of the sample. The lifetime mapping was measured in a high injection level.

shows the electron fluence of the irradiation employed in this study and the estimated Z<sub>1/2</sub> concentration in the irradiated samples. The electron fluence was adjusted so that each Z<sub>1/2</sub> concentration generated by irradiation energy of 200 keV and 400 keV becomes at a same level. Since the acceptor concentration of the p-type epilayers is  $5.6 \times 10^{14} \text{ cm}^{-3}$ , the estimated Z<sub>1/2</sub> concentration was adjusted in the range from  $4 \times 10^{13}$  to  $2 \times 10^{14} \text{ cm}^{-3}$  to avoid complete compensation of the epilayers.

Figure 6 shows the mapping of carrier lifetimes for the p-type 4H-SiC sample irradiated with an energy of 200 keV. In this figure, the irradiation conditions in the sample are shown in Fig. 6(a), and the lifetime mapping result is shown in Fig. 6(b). The distribution of carrier lifetime in each irradiated area is very uniform. The carrier lifetime in the p-type SiC can be varied in the range from 0.1 to 1.6 μs by electron irradiation.

#### IV. DISCUSSION

Figure 7 shows the relation between the inverse of carrier lifetime and the estimated Z<sub>1/2</sub> concentration in the irradiated samples with irradiation energy of 200 keV and

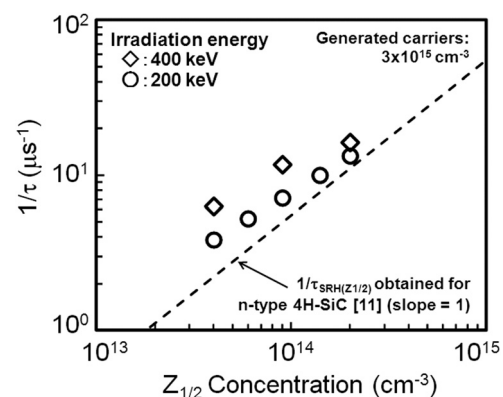


FIG. 7. Relation between the inverse of carrier lifetime and the estimated Z<sub>1/2</sub> concentration in irradiated p-type 4H-SiC. The dashed line in the figure is obtained from the measurements on n-type 4H-SiC.<sup>11</sup> The carrier lifetime was measured in a high injection level.

400 keV. From this figure, the inverse of carrier lifetime increases in proportion to the estimated  $Z_{1/2}$  concentration for the irradiation energy of 200 keV. In the case of 400 keV irradiation, the lifetime— $Z_{1/2}$  concentration relation is similar to the case for the irradiation energy of 200 keV. When the lifetimes of the samples irradiated with 200 keV and 400 keV are compared, the lifetime for 400 keV irradiation is close to, but slightly shorter than that for 200 keV irradiation at a given  $Z_{1/2}$  concentration. With respect to the irradiation energy, the carbon displacement in 4H-SiC is introduced at energies higher than 100 keV. On the other hand, the threshold energy for silicon displacement is about 250 keV.<sup>33</sup> The carrier lifetimes at a given  $Z_{1/2}$  concentration (estimated) do not depend on the irradiation energy (200 keV or 400 keV) very much. This result suggests that the lifetime killer in p-type 4H-SiC may be ascribed to a defect generated by carbon displacement.

For comparison purpose, the relation experimentally obtained for n-type 4H-SiC is included in Fig. 7 as denoted by a dashed line.<sup>6</sup> Regarding this line obtained for n-type 4H-SiC, the inverse of carrier lifetime is proportional to the  $Z_{1/2}$  concentration (slope = 1), suggesting that Shockley-Read-Hall (SRH) recombination via the  $Z_{1/2}$  center governs the lifetime. According to the SRH model, the bulk lifetimes should be the same for the p-type and n-type semiconductors with the same defect density in sufficiently high injection levels.<sup>34,35</sup> From this figure, the carrier lifetimes in electron-irradiated p-type SiC are close to the dashed line obtained for n-type SiC, being consistent with the SRH model.

This result suggests the possibility that the lifetime killer in p-type 4H-SiC could be the same as that in n-type 4H-SiC, namely, the  $Z_{1/2}$  center (at least at high injection level), although currently there is no direct evidence for this assignment. However, the slope for p-type 4H-SiC does not agree well with that for n-type material. This may be attributed to the influence of other recombination paths such as surface recombination, which should be different for n- and p-type 4H-SiC. In addition, the concentration of the  $Z_{1/2}$  center shown in Fig. 7 is not directly measured but assumed values, as described in Sec. III B. In p-type 4H-SiC, the charge state of the  $Z_{1/2}$  center will be different from that in n-type material and may be positively charged (donor-like level). We have performed DLTS measurements of p-type 4H-SiC epilayers up to 700 K, but any signatures of the donor-like level have not been observed so far. We speculate that the donor-like level may be energetically very deep from the valence band edge, and the DLTS peak will appear in the much higher temperature side.<sup>30</sup> Therefore, it is important to directly measure the  $Z_{1/2}$  concentrations in more detail in p-type 4H-SiC. When a lifetime killer is a monovalent defect, the SRH theory predicts that the lifetime should be the same in n- and p-type semiconductors with the same defect density. However, this is not always correct when the lifetime killer is multi-valent defect. Since the  $Z_{1/2}$  center actually takes multi charge states, the situation will be more complicated.<sup>36</sup> The charge state of a carbon vacancy, which may be an origin of the  $Z_{1/2}$  center, will be positive in p-type 4H-SiC. Therefore, the  $\text{EH}_{6/7}$  center, which may be the donor-like level of a

carbon vacancy, is an alternative candidate for the lifetime killer in p-type 4H-SiC. Anyway, it is difficult to give conclusive views at present, and the lifetime killer in p-type SiC should be further investigated. Provided that the lifetime killer in p-type 4H-SiC in the high injection level is the  $Z_{1/2}$  center as described above, the authors speculate the reason why the carrier lifetime is not much improved even after the thermal oxidation or carbon implantation process is employed, as in the next paragraph.

The origin of the  $Z_{1/2}$  and  $\text{EH}_{6/7}$  centers is recognized as being related to a carbon vacancy.<sup>37</sup> The model to explain trap reduction by thermal oxidation is described as follows:<sup>23,27</sup> Carbon and silicon interstitials are generated at the  $\text{SiO}_2/\text{SiC}$  interface by oxidation. The carbon interstitials, which mainly diffuse into the bulk, occupy the vacancies, resulting in the reduction of  $Z_{1/2}$  and  $\text{EH}_{6/7}$ . According to this model, the authors suggest two reasons why the carrier lifetime in p-type 4H-SiC after thermal oxidation is not much improved as that in n-type. One is the difference of carbon emission rate from the oxidizing interface for n- and p-type 4H-SiC, and the other is the difference of carbon diffusion in the epilayers. Regarding the carbon emission rate, the result of the carbon implantation with subsequent Ar annealing (Fig. 5) should be taken into account. In this case, the carrier lifetime was not much enhanced despite that a high density of carbon ions was directly implanted into the epilayers. Hence the difference of the carbon emission rate can be excluded in this case. As for the carbon diffusion, Bockstedte *et al.* have reported that migration barriers of interstitials strongly depend on the charge state, based on theoretical calculation using a density functional theory (DFT) in local density approximation (LDA).<sup>38</sup> The calculation shows that the migration barrier of a carbon interstitial in positive charge states (0.9–1.4 eV) is higher than that in negative charge states (0.6 eV). Thus, the diffusion of carbon interstitials in the p-type epilayers, where the interstitials will be positively charged, must be significantly smaller than that in the n-type epilayer, where the interstitials will be negative charged. This may be the reason why thermal oxidation and carbon implantation techniques are not so effective for enhancing the carrier lifetime in p-type SiC as in n-type SiC. However, we cannot exclude the possibility that a deep level other than the  $Z_{1/2}$  center may partly limit the carrier lifetime in p-type epilayers. It is thus important to elucidate the deep levels in p-type epilayers by DLTS and minority carrier transient spectroscopy (MCTS).

As for surface recombination, we attempted to reduce a surface recombination velocity in p-type 4H-SiC by employing the surface passivation with deposited  $\text{SiO}_2$  followed by annealing in NO, which is effective for lifetime enhancement in n-type 4H-SiC. The surface recombination velocity on p-type 4H-SiC, however, may be still high.<sup>39</sup> The distribution of surface state density must be different near the conduction and valence bands. In addition, the direction of surface band bending is opposite, and the position of the surface Fermi level must be different for n- and p-type epilayers. Quantitative evaluation of the surface recombination velocity for p-type SiC is a subject of future study.

## V. CONCLUSION

The authors have addressed the enhancement and control of carrier lifetimes in thick p-type 4H-SiC epilayers. Oxidation and subsequent Ar annealing combined with adequate surface passivation are effective in enhancing the carrier lifetimes in p-type 4H-SiC. The improvement of carrier lifetimes in p-type 4H-SiC has been confirmed not only by thermal oxidation but also by carbon implantation and subsequent Ar annealing, as in the case of n-type 4H-SiC. The carrier lifetimes in p-type SiC could be improved from 0.9  $\mu\text{s}$  (as-grown) to 2.6  $\mu\text{s}$  by thermal oxidation at 1350 °C for 45 h and subsequent Ar annealing at 1550 °C for 30 min, though an improvement effect of the carrier lifetime in p-type 4H-SiC is not as large as in n-type. The authors have speculated that insufficient elimination of the  $Z_{1/2}$  center may be responsible for the less-enhanced lifetime in the p-type epilayers.

The carrier lifetime in p-type 4H-SiC could be controlled from 0.1 to 1.6  $\mu\text{s}$  by employing the lifetime-enhanced epilayers and electron irradiation with irradiation energy of 200 keV or 400 keV. Uniform distributions of carrier lifetimes inside the irradiated areas have been confirmed from lifetime mapping. As a result of experiment, the inverse of the carrier lifetime is almost proportional to the estimated concentration of  $Z_{1/2}$  center generated by electron irradiation. In addition, the carrier lifetimes in the high injection level for p-type 4H-SiC are close to the lifetime— $Z_{1/2}$  concentration relationship experimentally obtained for n-type SiC, which is consistent with the SRH model.

## ACKNOWLEDGMENTS

This work was supported by the Funding Program for World-Leading Innovative R&D on Science and Technology (FIRST Program) and a Grant-in-Aid for Scientific Research (No. 21226008) from the Japan Society for the Promotion of Science, and the Global COE Program (C09) from the Ministry of Education, Culture, Sports, Science and Technology, Japan.

<sup>1</sup>H. Matsunami and T. Kimoto, *Mater. Sci. Eng. R* **20**, 125 (1997).

<sup>2</sup>J. A. Cooper, Jr., M. R. Melloch, R. Singh, A. Agarwal, and J. W. Palmour, *IEEE Trans. Electron Devices* **49**, 658 (2002).

<sup>3</sup>J. P. Bergman, O. Kordina, and E. Janzén, *Phys. Status Solidi A* **162**, 65 (1997).

<sup>4</sup>T. Tawara, H. Tsuchida, S. Izumi, I. Kamata, and K. Izumi, *Mater. Sci. Forum* **457–460**, 565 (2004).

<sup>5</sup>P. B. Klein, B. V. Shanabrook, S. W. Huh, A. Y. Polyakov, M. Skowronski, J. J. Sumakeris, and M. J. O'Loughlin, *Appl. Phys. Lett.* **88**, 052110 (2006).

<sup>6</sup>K. Danno, D. Nakamura, and T. Kimoto, *Appl. Phys. Lett.* **90**, 202109 (2007).

<sup>7</sup>S. A. Reshanov, W. Bartsch, B. Zippelius, and G. Pensl, *Mater. Sci. Forum* **615–617**, 699 (2009).

<sup>8</sup>L. Storasta and H. Tsuchida, *Appl. Phys. Lett.* **90**, 062116 (2007).

<sup>9</sup>T. Hiyoshi and T. Kimoto, *Appl. Phys. Express* **2**, 041101 (2009).

<sup>10</sup>P. B. Klein, *J. Appl. Phys.* **103**, 033702 (2008).

<sup>11</sup>T. Kimoto, K. Danno, and J. Suda, *Phys. Status Solidi B* **245**, 1327 (2008).

<sup>12</sup>T. Kimoto, T. Hiyoshi, T. Hayashi, and J. Suda, *J. Appl. Phys.* **108**, 083721 (2010).

<sup>13</sup>T. Miyazawa, M. Ito, and H. Tsuchida, *Appl. Phys. Lett.* **97**, 202106 (2010).

<sup>14</sup>M. Kato, M. Kawai, T. Mori, M. Ichimura, S. Sumie, and H. Hashizume, *Jpn. J. Appl. Phys., Part 1* **45**, 5057 (2007).

<sup>15</sup>T. Hayashi, K. Asano, J. Suda, and T. Kimoto, *J. Appl. Phys.* **109**, 014505 (2011).

<sup>16</sup>A. K. Agarwal, J. B. Casady, L. B. Rowland, S. Seshadri, R. R. Siergiej, W. F. Valek, and C. D. Brandt, *IEEE Electron Device Lett.* **18**, 518 (1997).

<sup>17</sup>Q. Zhang, M. Das, J. Sumakeris, R. Callanan, and A. K. Agarwal, *IEEE Electron Device Lett.* **29**, 1027 (2008).

<sup>18</sup>T. Kimoto, Y. Nanen, T. Hayashi, and J. Suda, *Appl. Phys. Express* **3**, 121201 (2010).

<sup>19</sup>P. B. Klein, R. Myers-Ward, K.-K. Lew, B. L. VanMil, C. R. Eddy, Jr., D. K. Gaskill, A. Shrivastava, and T. S. Sudarshan, *J. Appl. Phys.* **108**, 033713 (2010).

<sup>20</sup>K. Schroder, *Semiconductor Materials and Device Characterization*, 2nd ed. (John Wiley & Sons, New York, 2006), Chap. 7.

<sup>21</sup>S. G. Sridhara, T. J. Eperijesi, R. P. Devaty, and W. J. Choyke, *Mater. Sci. Eng. B* **61–62**, 229 (1999).

<sup>22</sup>A. Koizumi, J. Suda, and T. Kimoto, *J. Appl. Phys.* **106**, 013716 (2009).

<sup>23</sup>T. Hiyoshi and T. Kimoto, *Appl. Phys. Express* **2**, 091101 (2009).

<sup>24</sup>N. Noborio, J. Suda, S. Beljakowa, M. Krieger, and T. Kimoto, *Phys. Status Solidi A* **206**, 2374 (2009).

<sup>25</sup>L. Storasta, H. Tsuchida, T. Miyazawa, and T. Ohshima, *J. Appl. Phys.* **103**, 013705 (2008).

<sup>26</sup>K. Kawahara, M. Krieger, J. Suda, and T. Kimoto, *J. Appl. Phys.* **108**, 023706 (2010).

<sup>27</sup>K. Kawahara, J. Suda, and T. Kimoto, *J. Appl. Phys.* **111**, 053710 (2012).

<sup>28</sup>T. Miyazawa, M. Ito, and H. Tsuchida, presented at ICSCRM2011, Cleveland, Ohio, 11–16 September 2011, We-1B-1.

<sup>29</sup>B. Zippelius, J. Suda, and T. Kimoto, *J. Appl. Phys.* **111**, 033515 (2012).

<sup>30</sup>K. Danno and T. Kimoto, *J. Appl. Phys.* **101**, 103704 (2007).

<sup>31</sup>T. Dalibor, G. Pensl, H. Matsunami, T. Kimoto, W. J. Choyke, A. Schöner, and N. Nordell, *Phys. Status Solidi A* **162**, 199 (1997).

<sup>32</sup>H. Kaneko and T. Kimoto, *Appl. Phys. Lett.* **98**, 262106 (2011).

<sup>33</sup>J. W. Steeds, F. Carosella, G. A. Evans, M. M. Ismail, L. R. Danks, and W. Voegeli, *Mater. Sci. Forum* **353–356**, 381 (2001).

<sup>34</sup>R. N. Hall, *Phys. Rev.* **87**, 387 (1952).

<sup>35</sup>W. Shockley and T. Read, Jr., *Phys. Rev.* **87**, 835 (1952).

<sup>36</sup>J. S. Blakemore, *Semiconductor Statistics* (Dover, NY, 1987), Chap. 8.

<sup>37</sup>L. Storasta, J. P. Bergman, E. Janzén, A. Henry, and J. Lu, *J. Appl. Phys.* **96**, 4909 (2004).

<sup>38</sup>M. Bockstedte, A. Mattausch, and O. Pankratov, *Phys. Rev. B* **69**, 235202 (2004).

<sup>39</sup>T. Hayashi, K. Asano, J. Suda, and T. Kimoto, *J. Appl. Phys.* **109**, 114502 (2011).